

Swelling Behavior of Thin, Surface-Attached Polymer Networks

Ryan Toomey, Daniel Freidank, and Jürgen Rühle*

Institute for Microsystem Technology, University of Freiburg, Georges-Köhler-Allee 103, D-79110 Freiburg, Germany

Received June 2, 2003; Revised Manuscript Received October 3, 2003

ABSTRACT: The swelling behavior of thin, surface-attached cross-linked dimethylacrylamide (DMAAm) films in contact with water has been characterized with multiple-angle nulling ellipsometry and compared to the swelling of nonattached, bulk DMAAm networks. The polymer networks are fabricated by cross-linking thin films of statistical copolymers composed of DMAAm and a photoreactive benzophenone derivative monomer. Covalent attachment of the film to the surface is achieved by means of a benzophenone-based silane monolayer. UV illumination simultaneously cross-links and chemically links the layer and chemically links the layer to the surface, forming stable networks that do not delaminate upon swelling. It is observed that the surface-attached networks swell less than the nonattached, bulk networks at the same cross-link density; however, the swelling of surface-attached networks is larger than that suggested by simple geometric considerations for swelling in one dimension. The results are in qualitative agreement with Flory–Rehner theory extended to one-dimensional swelling.

Introduction

Thin layers of surface-attached polymer networks offer a powerful route toward soft surfaces with well-defined mechanical, physical and biochemical properties.^{1–4} First, polymer networks provide a soft 3-dimensional scaffold capable of hosting a wide-array of functionalities, ranging from proteins to inorganic nanoparticles. Second, polymer networks can undergo substantial swelling and contraction in response to specific stimuli,^{5–8} making them excellent candidates for “smart” surfaces with sensing and actuating characteristics. While macroscopic gels have been hindered by slow response times, the collective diffusion of the network is the rate-limiting step; therefore, reducing their dimensions to the microscale should significantly enhance performance, making them especially attractive in microsystems technology.^{9,10}

A critical issue for understanding and predicting the properties of surface-attached polymer networks is the impact of confinement on their swelling behavior.¹¹ Chemical linkage of the network to a surface prevents swelling parallel to the substrate, effectively confining the volume change to one dimension, or normal to the surface. Such an effect will impact important properties such as the structure, mechanical properties, dynamics, and permeability of the network. It has already been observed that confinement of *N*-isopropylacrylamide (NIPAM) networks raises the volume phase transition temperature in comparison to that with unconfined networks.^{7,12} Furthermore, it was recently reported that surface-attached NIPAM gels have a total volume change around 15-fold while the corresponding bulk gels have experienced a volume change as large as 100-fold.^{13,14} For isotropic, neutral networks, the widely applied Flory–Rehner theory has met with some success in describing the relationship between the cross-link density and the equilibrium swelling in a good solvent.^{15,16} For sufficiently low cross-link densities, the Flory–Rehner theory predicts that the equilibrium swelling of a gel scales as the cross-link density to the

$-3/5$ power. However, as surface-attachment restricts the swelling to one dimension, a smaller dependence is expected on the cross-link density.

In this paper, we use a simple photochemical technique for producing surface-attached polymer networks. The fabrication approach is based on the photocross-linking of films of statistical copolymers comprising methacryloyloxybenzophenone (MaBP) and dimethylacrylamide (DMAAm). Irradiation of the DMAAm–MABP films with UV light ($\lambda = 350$ nm) triggers the n,π^* transition in the MaBP segments, leading to a biradical triplet state that is capable of abstracting a hydrogen from almost any kind of neighboring aliphatic C–H group, forming a stable C–C bond.¹⁷ The approach can be used with essentially any technique of film formation which yields thin coatings of controllable thickness (e.g., spin or dip casting).

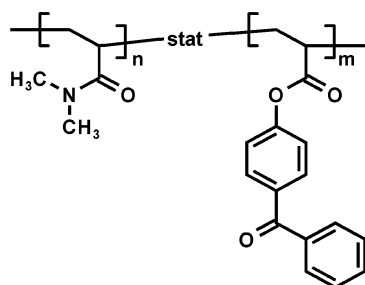
The swelling behavior of the surface-attached DMAAm–MaBP layers was characterized with multiple-angle null ellipsometry in an ATR configuration, an analytical technique that yields information about the thickness and refractive index profile of the swollen layer.¹⁸ Ellipsometric measurements reveal that the swelling degree of the surface-attached networks is related to the MaBP content in the layer, which can be varied by one of two methods. In the first, the MaBP fraction in the copolymer can be controlled during the synthesis, i.e., by adjusting the ratio of the two monomer concentrations in the monomer feed during the polymerization process. In the second method, the cross-link density can be controlled by blending DMAAm–MaBP copolymer with DMAAm homopolymer.

In addition to the generation of the surface-attached gels, the corresponding nonattached bulk gels were prepared under identical conditions and compared to the swelling of the surface-attached gels to understand the effect of confinement on their swelling behavior.

Experimental Section

DMAAm–MaBP Synthesis. A series of DMAAm–MaBP copolymers was synthesized by statistical free-radical copolymerization of *N,N*-dimethylacrylamide monomer (Aldrich) and 4-methacryloyloxybenzophenone (MaBP) monomer. The

* Corresponding author. E-mail: ruehe@imtek.uni-freiburg.de.

Chart 1. Chemical Structure of the DMAAm-MaBP Polymers**Table 1. Chemical Compositions of the DMAAm-MaBP Polymers**

content of MaBP (mol %)		mol wt M_w	polydispersity M_w/M_n
feed	polymer		
0.0	0.0	1056 000	2.4
0.5	not detectable	155 000	2.5
1.0	1.0	113 000	3.3
3.0	3.6	92 800	3.0
10.0	14.3	134 000	5.4

structure of the polymers are shown in Chart 1. The polymerization was initiated using 0.1% α, α' -azoisobutyronitrile (AIBN), and the reactions were carried out at 60 °C for 15 h in DMF under nitrogen after degassing the reaction mixtures by three freeze and thaw cycles. The polymer was purified by double precipitation in diethyl ether, typically yielding approximately 65% of a white powder. The MaBP monomer was synthesized from 4-hydroxybenzophenone and methacryloyl chloride via a typical esterification reaction in dichloromethane solvent and triethylamine as the acid scavenger. The properties of the polymers are listed in Table 1. For characterization, the ^1H NMR spectra were recorded on a Bruker MSL 300 spectrometer (300 MHz). The molecular weight M_w and the molecular weight distribution (polydispersity M_w/M_n) of the copolymers were determined by gel-permeation chromatography with an Agilent instrument equipped with an RI detector and software from PSS.

Surface-Attached Network Preparation. Thin DMAAm-MaBP copolymer films were prepared by dip-coating LaSFN9 prisms (Hellma, Germany) in DMAAm-MaBP/2-propanol solutions. The 2-propanol content was adjusted to yield films of approximately 100 nm in thickness. Before dip-coating, the prisms were activated in 1 M sulfuric acid for 1 min and rinsed thoroughly in Millipore water and ethanol. To aid in the attachment of the polymer network to the prism surface, a benzophenone-based silane (4-(3'-chlorodimethylsilyl)propyloxybenzophenone) was immobilized at the surface.¹⁹ The samples were dried under nitrogen and irradiated under a high pressure mercury lamp for 30 min. Immediately after UV illumination, the samples were characterized with ellipsometry.

Characterization of the Surface-Attached Networks. The dry and swollen profiles of the surface-attached films were measured with a home-built variable-angle nulling ellipsometer in an ATR configuration. The light-source was a He-Ne laser with a wavelength of $\lambda = 633$ nm. The experimental setup has been described in detail elsewhere.¹⁸ The refractive index of the LaSFN9 prism is $n = 1.845$, and in contact with water the critical angle of total reflection is 46.3°. The main features used for analysis of the ellipsometry data occur close to the critical edge, and so angular scans of the samples were taken between 40 and 55° with 0.1° increments. The thickness of all films were in the optical range, giving rise to sufficient features in the recorded spectra to infer the refractive index profile. To analyze the data, model refractive index profiles were generated, and the ellipsometric parameters were numerically calculated using the matrix optical formulation.²⁰ The parameters of the model were adjusted to minimize the differences between the simulation and experimental data. The polymer

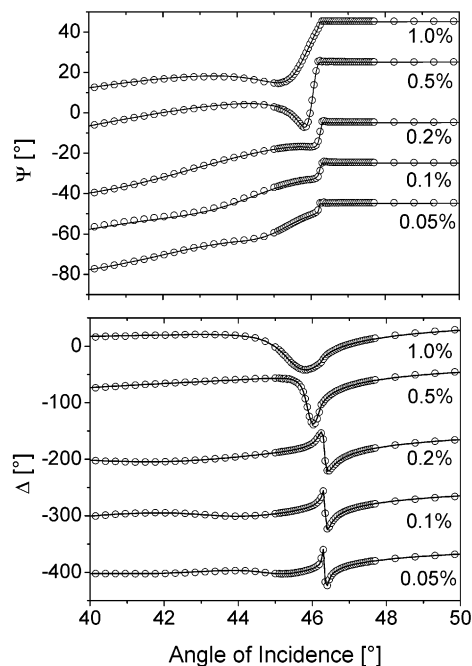


Figure 1. Representative ellipsometry delta and psi scans against the angle of incidence for a series of DMAAm surface-attached networks. The percentage of MaBP corresponds to the average molar concentration of the cross-linkable monomer in the network. All dry thicknesses were approximately 100 nm. The continuous lines represent the best fits with the structural profiles shown in Figure 3.

volume fraction $\phi(z)$ was determined from the refractive index profile $n(z)$ with the Lorentz-Lorenz equation using an effective medium approximation:²¹

$$\phi(z) = \left(\frac{n_{\text{solvent}}^2 - n_0^2}{n_{\text{solvent}}^2 + 2n_0^2} \right) \left(\frac{n(z)^2 - n_0^2}{n(z)^2 + 2n_0^2} \right) \quad (1)$$

where n_0 is the refractive index of the polymer and n_{solvent} is the refractive index of the solvent.

Results and Discussion

The equilibrium swelling of the surface-attached DMAAm networks was measured for a series of MaBP concentrations, where the average molar MaBP fraction was varied over 2 orders of magnitude, from 0.05% to 10%. The MaBP content was controlled by one of two methods. In the first method, the MaBP molar fraction was varied in the synthesis of the DMAAm-MaBP copolymer. In the second method, DMAAm-MaBP(1%) copolymer with 1% MaBP molar content was blended with DMAAm homopolymer, where the molecular weight of the DMAAm homopolymer is approximately an order of magnitude larger than the DMAAm-MaBP copolymer. The latter method also leads to stable networks provided that the molecular weights and blending ratio between the two polymers are chosen appropriately. Blending offers a simple route to adjust the cross-link density without the need to synthesize a new polymer each time to tune the equilibrium swelling of the network.

Figure 1 shows the measured ellipsometry Ψ and Δ pairs for a series of the surface-attached DMAAm networks as a function of MaBP content in contact with aqueous solution. The MaBP content in each of the samples was controlled by blending DMAAm homopolymer and DMAAm-MaBP(1%). The data are reported

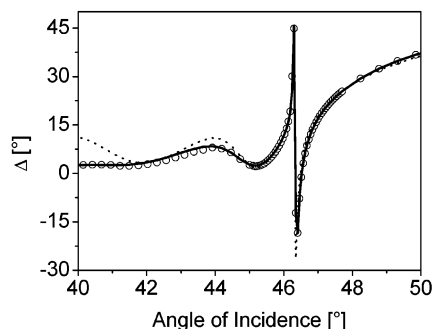


Figure 2. Ellipsometry delta scan for the 0.05 mol % DMAAm-MaBP sample with the best fit for a two-parameter box-model (dashed line) and a three-parameter error-function model (solid line).

in terms of the average MaBP molar ratio in the layer. The dry layer thickness of each sample was approximately 100 ± 10 nm with a refractive index of 1.51 ± 0.02 , as measured by ellipsometry. Immediately after the dry layer measurement, water was added to the cell and the transition to the final swollen state was monitored. In all cases, the swelling kinetics was relatively fast, occurring in less than 30 s, which is the time needed for a single measurement. All measurements produced constant readings in Ψ and Δ immediately following exposure to water.

Inspection of the ellipsometric spectra in Figure 1 shows significant changes in both the ellipsometric Δ and Ψ scans as the average MaBP content is decreased, corresponding to an expansion of the profile with decreasing cross-link density. To model the swollen films, initially a simple box-model with a uniform polymer volume fraction was used; however, reasonable fits were found only at sufficiently high MaBP content. As the MaBP content was decreased, the uniform layer model no longer adequately described the swollen profile. For instance, Figure 2 shows the Δ scan for the 0.05% MaBP sample modeled with the uniform box profile, denoted by the dashed line. While the simulation captures most of the features of the experimental data, the simulation shows a more pronounced oscillation in Δ at low incidence angles than the experimental data. The fit at low angles could be consequently improved by permitting roughness at the outer edge of the profile, which dampens the low angle oscillation in the simulation while preserving the remaining features of the curve. It was assumed the roughness is described by an error function, thus the profile was modeled as

$$\phi(z) = \left(\frac{\phi_e}{2}\right) \left[1 - \left\{ \operatorname{erf} \left(\frac{z - L_e}{\sigma} \right) \right\} \right] \quad (2)$$

where ϕ_e is the average polymer volume fraction in the layer, L_e is the central position of the interface, and σ is the width of the interface. The solid line in Figure 2 corresponds to the improved fit using the box model with an error-type interface, involving three adjustable parameters altogether. More sophisticated models were not considered as the data do not have sufficient structural sensitivity to justify their use.

Figure 3 shows the volume fraction profiles which best describe the 1% MaBP, 0.2% MaBP, and the 0.05% MaBP swollen layers using the aforementioned three-parameter model. For the 1% MaBP case, the data could be fit with the absence of an interface ($\sigma \approx 0$ nm). For the 0.2% MaBP and the 0.05% MaBP samples, the

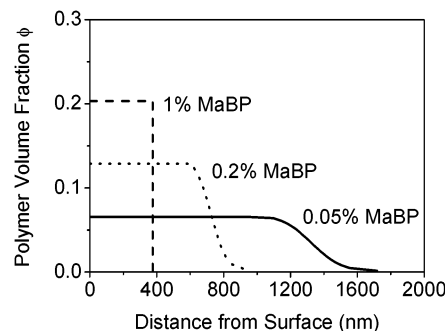


Figure 3. Polymer fraction profiles that represent the fits in Figure 1 for the 1%, 0.2%, and 0.05 mol % DMAAm-MaBP samples.

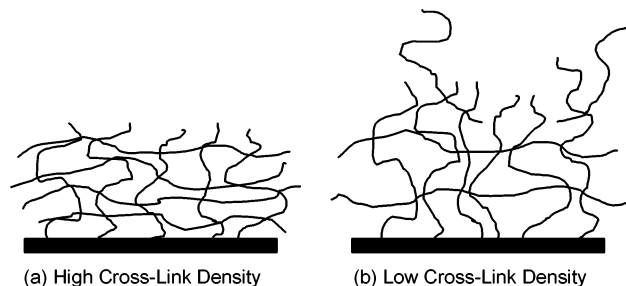


Figure 4. Cartoon depicting the swollen structure of the surface-attached polymer network at high (a) and low cross-link densities (b). At sufficiently low cross-link density, peripheral chains are more likely to penetrate into the solvent giving rise to a more diffuse interface.

interfacial width took on values of $\sigma = 100$ nm and $\sigma = 200$ nm, respectively. While a finite interface width is expected under all conditions, features much less than the wavelength of light cannot be resolved with ellipsometry. The estimated precision in the interface width is ± 50 nm. The physical explanation for the interface stems from a small number of chains that extend beyond the network. The outer edge of the layer becomes rougher at lower cross-link densities since the polymer chains are not as tightly confined to the interface and can more easily penetrate into the solvent, as shown in Figure 4. It is suspected that the interface width is a strong function of the molecular weight of the individual polymer chains; however, this effect was not studied in the present experiments.

From the model fits, both the average thickness L_e and the average polymer volume fraction ϕ_e in the swollen layers were independently determined. Therefore, two quantities can be calculated that characterize the swelling of the layer:

$$\alpha = \frac{L_e}{L_0} \quad (3)$$

where α measures the linear swelling in the direction perpendicular to the surface. The thickness L_0 represents thickness of the dry film. Furthermore,

$$S = \frac{\phi_0}{\phi_e} \quad (4)$$

where S is the volumetric swelling degree in the gel, and ϕ_0 represents the volume fraction occupied in the prepared state. If the attached networks swell only perpendicularly to the surface with no swelling parallel to the surface, then the linear degree of swelling α and

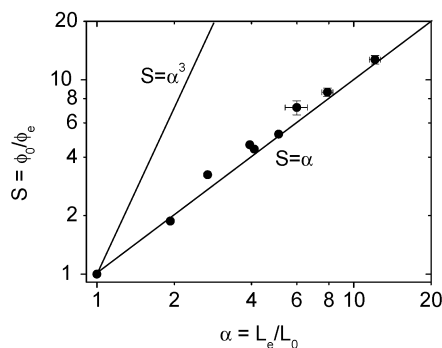


Figure 5. The linear degree of swelling α versus the volumetric degree of swelling S for a series of surface-attached DMAAm-MaBP networks. The solid lines represent the relationship between the two quantities if the surface-attached networks undergo pure uniaxial swelling ($S = \alpha$) and swelling in three dimensions ($S = \alpha^3$).

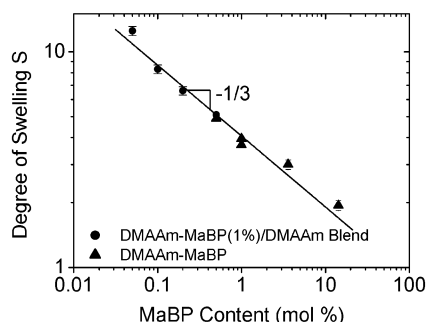


Figure 6. Average degree of swelling S vs the MaBP content for a series of DMAAm surface-attached networks. As denoted by the symbol, the MaBP content was varied either through the synthesis conditions of the DMAAm-MaBP copolymer (\blacktriangle) or by blending DMAAm homopolymer with DMAAm-MaBP(1%) (\bullet). The solid line corresponds to a best fit power-law $S \propto [\text{MaBP content}]^{-1/3}$.

the volumetric degree swelling S must be necessarily equal, in other words

$$\frac{L_e}{L_0} = \frac{\phi_0}{\phi_e} \quad (5)$$

Figure 5 shows a logarithmic plot of S vs α for a series of DMAAm-MaBP surface-attached networks with swell ratios S between approximately 2 and 12. Also shown are two trendlines corresponding to $S = \alpha$ and $S = \alpha^3$, which represent swelling in one dimension and three dimensions, respectively. Since the uncertainty in the measurement and model fits leads to approximately a 10% precision in the degree of swelling calculated with either method, it therefore it can be concluded that within the experimental error of the experiment, $S = \alpha$, and the layers are undergoing pure uniaxial extension normal to the surface.

Figure 6 shows the relationship between the volumetric swelling degree S of the surface-attached layers and the average MaBP content in the layer. The samples were produced by either blending DMAAm homopolymer/DMAAm-MaBP(1%) copolymer or by directly altering the MaBP content in the copolymer, as denoted by the symbol in the figure. It is remarkable to note that all the samples follow a general trend with respect to the average MaBP content. To a first approximation, it is expected that the degree of swelling S should not only depend on the average cross-link density, but also on the topological distribution of those

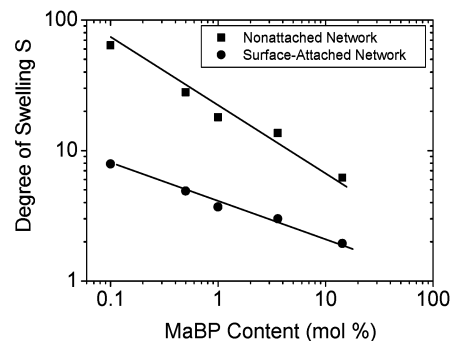


Figure 7. Comparison of the overall degree of swelling between the surface-attached (\bullet) and unconstrained bulk DMAAm networks (\blacksquare).

cross-links. Since blending would be expected to alter the cross-link distribution, it is reasonable to expect a difference in the behavior of both systems; however, this effect may be small, and in order to confirm the effect, a much more exhaustive study would have to be conducted. For the blended samples, when the average MaBP content was reduced below 0.05%, the networks were no longer stable and delaminated from the surface upon exposure to water, effectively limiting the range of MaBP contents that could be measured. The trend line corresponds to a best fit slope of $-1/3$, suggesting that the swell ratio of the surface-attached network scales as approximately the cube root of the number of segments between cross-links.

To explore the significance of this scaling dependence of the surface-attached DMAAm networks, the equivalent bulk networks were prepared using the same preparation conditions. In each case, approximately 0.05 g of the polymer was deposited to a glass substrate from chloroform forming a layer approximately 500 μm thick. The layers were thoroughly dried under vacuum and then UV irradiated for 30 min, the same irradiation time as for the surface-attached gels. The layers were then exposed to water. As they swelled, they eventually delaminated from the glass surface and were allowed to reach equilibrium (approximately 1 week). The swollen gels were then weighed and their degree of swelling was defined as $S = m_e/m_0$ where $m_{e,0}$ is the mass of the polymer gel in the equilibrium swollen state and dry state, respectively. Assuming the density of the dry DMAAm network is close to 1, the degree of swelling as determined by weighing the wet and dry gels corresponds to the definition of eq 4.

Figure 7 shows a comparison of the volumetric degree of swelling S as a function of MaBP content for both the surface-attached and the nonattached gels. It is readily seen that the nonattached networks swell to a much higher degree than the surface-attached networks at all cross-link densities. As the nonattached networks can swell isotropically, this observation is consistent with the idea that higher degrees of freedom permit the network to swell to a greater extent than a gel that is mechanically or physically constrained. For the nonattached gel, the degree of swelling in all three dimensions is presumed to be equal, $\alpha_x = \alpha_y = \alpha_z$, where α_i is the linear deformation L_e/L_0 in the i direction. Therefore, by constraining the network to the surface, from simple geometric considerations, it may be expected that the degree of swelling of the surface-attached network will be the cube root of the unconstrained network, or $S_{sa} = S_{uc}^{1/3}$. For example, at 0.1 mol % MaBP, the unconstrained network swells approximately 64 times. It then

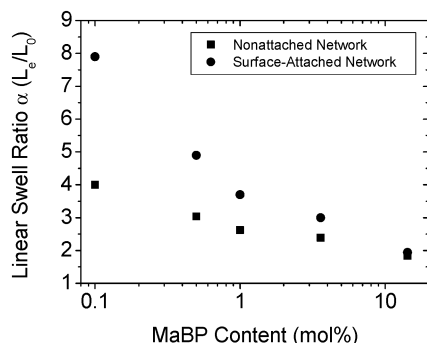


Figure 8. Comparison of the linear degree of swelling α between the surface-attached (●) and nonattached (■) DMAAm networks. The value α for the nonattached networks is approximated as the cube root of their average degree of swelling, $\alpha = S^{1/3}$.

may be expected that the surface-attached network should only swell by a factor of $(64)^{1/3} = 4$. However, the surface-attached gel swells to approximately 8 times its dry thickness, much larger than expected by this simple relationship.

Figure 8 compares the linear swelling degree of the unconstrained networks $\alpha_{uc} = S_{uc}^{1/3}$ with the linear swelling degree α_{sa} for the surface-attached networks. It is consistently observed that the linear swelling degree of the surface-attached networks exceeds the linear swelling degree of the nonattached networks, becoming more pronounced at the lowest cross-link densities. This observation can be understood by a simple phenomenological model based on a Flory-type expression for the free energy.²² Upon immersion in a good solvent, the equilibrium structure of a polymer network is subject only to two opposing forces: the thermodynamic force of mixing, which favors swelling, and the elastic retractile force of the network, which opposes swelling. The free energy of the system can be written as

$$\Delta G = \Delta G_{\text{mix}} + \Delta G_{\text{elastic}} \quad (6)$$

The mixing free energy is

$$\frac{\Delta G_{\text{mix}}}{kT} = n_1 \ln(1 - \phi) + \chi n_1 \phi \quad (7)$$

where k is the Boltzmann constant, T is the absolute temperature, n_1 is the number of solvent molecules, ϕ is the polymer fraction in the swollen gel, and χ is the Flory polymer–solvent interaction parameter. The expression for the elastic free energy is

$$\frac{\Delta G_{\text{elastic}}}{kT} = \nu \left(\frac{d}{2} \right) [\alpha^2 - 1 - \ln \alpha] \quad (8)$$

where ν is the number of cross-links in the network and d is the number of dimensions in which the network can swell. Noting that the polymer volume fraction ϕ in the swollen network is related to its linear deformation α through

$$\phi = \frac{\phi_0}{\alpha^d} \quad (9)$$

Minimization of the free energy ΔG of the swollen network yields the following relationship between the equilibrium linear deformation α and the degrees of

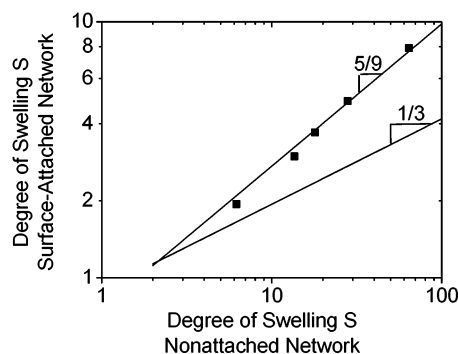


Figure 9. Log–log plot showing the relationship between the volumetric swelling degree S for surface-attached and nonattached DMAAm networks prepared under identical conditions. The degree of swelling in the surface-attached networks scales as the $5/9$ power of the degree of swelling in the nonattached networks, in qualitative agreement with the extension of Flory–Rehner theory to one-dimension. A $1/3$ power-law relationship from simple geometric arguments is also plotted for comparison.

freedom in which the network can swell:

$$\alpha \approx \left[\frac{1}{(\phi_0^{1/2} - \chi)\phi_0 N_c} \right]^{-1/(d+2)} \quad (10)$$

As swelling is confined to fewer dimensions, α shows a stronger dependence on the cross-link density $1/N_c$, where N_c is the number of segments between cross-links. Since the volumetric swelling degree $S = \alpha^d$, the dependencies of both S and α can be determined for three-dimensional and one-dimensional swelling in a good solvent:

$$\alpha_{uc} \approx \left(\frac{1}{\phi_0 N_c} \right)^{-1/5} \quad S_{uc} \approx \left(\frac{1}{\phi_0 N_c} \right)^{-3/5} \quad [\text{unconstrained}] \quad (11)$$

and

$$\alpha_{sa} \approx \left(\frac{1}{\phi_0 N_c} \right)^{-1/3} \quad S_{sa} \approx \left(\frac{1}{\phi_0 N_c} \right)^{-1/3} \quad [\text{surface-attached}] \quad (12)$$

The experimental observations presented in Figure 8, wherein the surface-attached networks show greater linear deformation than the equivalent unconstrained networks, can be qualitatively understood within the context of the presented model. As surface attachment limits swelling to one dimension, the polymer concentration in a surface-attached network is still a factor α^2 greater than in the equivalent unconstrained network at the same linear extension α . Consequently, the surface-attached network experiences a higher mixing osmotic pressure, which is partially relieved by further extension in its swelling direction, thus leading to a higher linear swelling ratio than possible in the unconstrained network. Equations 11 and 12 predict that the volumetric degree of swelling in the surface-attached network should be approximately the square root of the degree of swelling in the unconstrained network:

$$S_{sa} = S_{uc}^{5/9} \quad (13)$$

Figure 9 shows this dependency superimposed on a plot of S_{sa} vs S_{uc} for the series of the DMAAm–MaBP

polymers shown in Figure 7, along with a simple cube root relationship. As already discussed, the cube root relationship stemming from simple geometric considerations does not adequately describe the experimental data, which are better described by the dependence given in eq 13. It should be noted that the model predicts a numerical prefactor of unity in eq 13, which overpredicts the observed experimental results by about 25%. This small discrepancy may have a number of causes. First, it was assumed that the specific density of the dry network was the same as water, which would lead to an overestimate of the volumetric degree of swelling S_{uc} for the nonattached networks from its mass if the specific density is less than water. Second, while it has been found that the volumetric swelling degree of isotropic networks in a good solvent is well described by $S = pN_c^{3/5}$, the slope p cannot be correctly predicted with the Flory–Rehner model.²³ It has been argued that the free energy expression for network swelling must be connected to the physical structure of the gel, which may lead to different expressions of the prefactor p in the unconstrained and constrained swelling cases.

Conclusions

Chemically attaching a polymer network to a surface reduces the degrees of freedom in which the network can swell, affecting its swollen internal structure. This work establishes a first step to understanding the effect of surface-attachment on the equilibrium structure of neutral polymer networks, providing a basis to interpret and predict the properties of hydrogels in confined environments. For instance, the mobility and diffusion of a guest species or a target signal within a polymer network and the dynamic response of that network is intimately tied to the internal structure of the network. Surface-attached polymer networks are expected to find considerable use in microfluidic devices, a rapidly expanding field, due to the tremendous design flexibility unique to polymers. Cross-linked polymer structures should permit a broad range of autonomous chemical sensing, fluid regulating, and mechanical actuating components in microfluidic systems.

Acknowledgment. This work has been supported by the DFG in the framework of the SFB428 (“Strukturierte Makromolekulare Netzwerksysteme”).

Supporting Information Available: Text giving a detailed mathematical derivation of eq 10. This material is available free of charge via the Internet at <http://pubs.acs.org>.

References and Notes

- (1) Revzin, A.; Russell, R. J.; Yadavalli, V. K.; Koh, W.-G.; Deister, C.; Hile, D. D.; Mellott, M. B.; Pishko, M. V. *Langmuir* **2011**, *17*, 5440.
- (2) Sanford, M. S.; Charles, P. T.; Commisso, S. M.; Roberts, J. C.; Conrad, D. W. *Chem. Mater.* **1998**, *10*, 1510.
- (3) Tang, Y.; Lu, J. R.; Lewis, A. L.; Vick, T. A.; Stratford, P. W. *Macromolecules* **2001**, *34*, 8768.
- (4) Kuckling, D.; Harmon, M. E.; Frank, C. W. *Macromolecules* **2002**, *35*, 6377.
- (5) Tanaka, T.; Nishio, I.; Sun, S.-T.; Ueno-Nishio, S. *Science* **1982**, *218*, 467.
- (6) Siegel, R. A. *Adv. Polym. Sci.* **1993**, *109*, 233.
- (7) Suzuki, A.; Kojima, S. *J. Chem. Phys.* **1994**, *101*, 10003.
- (8) Qui, Y.; Park, K. *Adv. Drug Delivery Rev.* **2001**, *53*, 321.
- (9) Zhao, B.; Moore, J. S. *Langmuir* **2001**, *17*, 4758.
- (10) Beebe, D. J.; Moore, J. S.; Bauer, J. M.; Yu, Q.; Liu, R. H.; Devadoss, C.; Jo, B.-H. *Nature (London)* **2000**, *404*, 588.
- (11) Onuki, A. *Adv. Polym. Sci.* **1993**, *109*, 63.
- (12) Harmon, M. E.; Kuckling, D.; Frank, C. W. *Macromolecules* **2003**, *36*, 162.
- (13) Seelenmeyer, S.; Deike, I.; Rosenfeldt, S.; Norhausen, C.; Dingenouts, N.; Ballauf, M.; Narayanan, T.; Linder, P. *J. Chem. Phys.* **2001**, *114*, 10471.
- (14) Harmon, M. E.; Jakob, T. A. M.; Knoll, W.; Frank, C. W. *Macromolecules* **2002**, *35*, 5999.
- (15) Flory, P. J.; Rehner, J. *J. Chem. Phys.* **1943**, *11*, 521.
- (16) Flory, P. J. *J. Chem. Phys.* **1950**, *18*, 108.
- (17) Turro, N. J. *Modern Molecular Photochemistry*; University Science Books: Mill Valley, CA, 1991.
- (18) Habicht, J.; Schmidt, M.; Ruehe, J.; Johannsmann, J. *Langmuir* **1999**, *15*, 2460.
- (19) Prucker, O.; Naumann, C. A.; Ruehe, J.; Knoll, W.; Frank, C. W. *J. Amer. Chem. Soc.* **1999**, *121*, 8766.
- (20) Azzam, R. M.; Bashara, N. M. *Ellipsometry and Polarized Light*; Elsevier: Amsterdam, 1987.
- (21) Born, M.; Wolf, E. *Principles of Optics*; University Press: Amsterdam, 1997.
- (22) Flory, P. J. *Principles of Polymer Chemistry*; Cornell University Press: Ithaca, NY, 1953.
- (23) Hild, G. *Polymer* **1997**, *13*, 3279.

MA034737V